Transformation optics on a silicon platform

Lucas H Gabrielli[1] and Michal Lipson[1,2]

[1] Cornell Nanophotonics Group, School of Electrical and Computer Engineering,
Cornell University, Ithaca, NY 14853, USA
[2] Kavli Institute at Cornell for Nanoscale Science, Cornell University, Ithaca, NY 14853, USA

E-mail: ml292@cornell.edu

Abstract

Transformation optics allows the creation of innovative devices; however, its implementation in the optical domain remains challenging. We describe here our process to design and fabricate such devices using silicon as a platform for broad band operation in the optical domain. We discuss the approximations and methods employed to overcome the challenges of using dielectric materials as a platform for transformation optics, such as the anisotropy and gradient refractive index implementation. These encompass conformal and quasi-conformal mappings, and a dithering process to discretize and quantize the continuously inhomogeneous index function. We show examples of devices that we fabricated and tested, including the carpet invisibility cloak, a broad bandwidth light concentrator, and a perfect imaging device, known as Maxwell's fish eye lens. Finally, we touch on future directions under investigation to further develop transformation optics based on dielectric materials.

Keywords: transformation optics, cloaking, light focusing, silicon photonics, nanofabrication

1. Introduction

Transformation optics (TO) reveals that the geometry of space and its constitutive parameters (i.e., permittivity and permeability tensors) affect electromagnetic waves equivalently [1–6]. In reality TO allows the implementation of virtual geometries in the real universe through specially designed, inhomogeneous dielectrics. For a few years now, this design capability brought about innovative devices, such as invisibility cloaks [7–11], and sub-diffraction limited imaging [12–17].

Nonetheless, despite their interesting characteristics, only a few of these designs were actually fabricated due to the challenging material requirements [9–11, 16–18]. Because TO generally creates devices with continuous, highly inhomogeneous constitutive parameters, their fabrication must be precisely controlled on the scale of the wavelength. To date one of the best platforms for TO has been based on meta-materials, which cannot yet be well-controlled and sufficiently fine grained in the optical regime.

In view of this deficiency in the fabrication of meta-materials, we choose silicon as a platform for TO. Silicon has a high refractive index contrast relative to both air and SiO$_2$, which allows for a reasonably wide range of parameters. The fabrication is CMOS compatible and is therefore based on a very mature and highly controllable fabrication platform. Additionally, being a transparent dielectric, silicon has no intrinsic absorption and, because we do not rely on any resonances, the fabricated devices operate over a broad wavelength bandwidth.

In this paper we present our advances in TO design and fabrication processes, and show examples of devices implemented using these techniques. We also discuss future directions that are being investigated to further develop TO using silicon as a platform.

2. Silicon platform

Devices created based on TO design have no reflecting boundaries and are, in general, composed of an anisotropic medium, in which different components of light experience different permittivities and permeabilities. Mathematically, the relative permittivity and permeability of the medium have a non-trivial, identical tensorial form: $\bar{\bar{\varepsilon}}' = \bar{\bar{\mu}}'$. The controlled
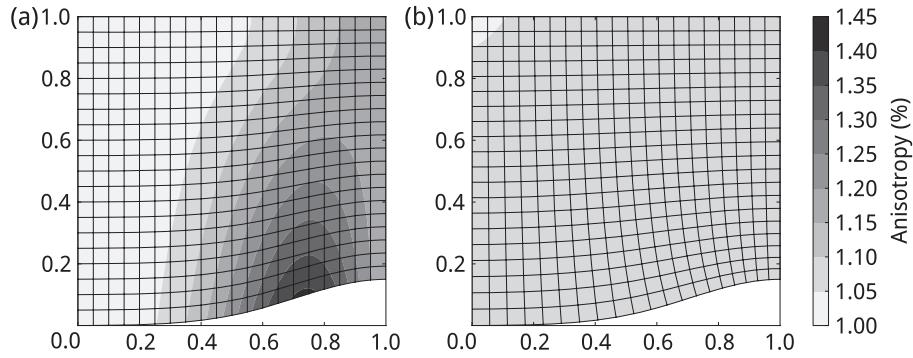
Figure 1. Example of anisotropy minimization (measured as the ratio between the maximal to the minimal refractive indices along the two principal axes of the medium [7]). Here we transform a square space in the one defined by the boundaries in the figures. The grid lines show how a square grid in the original space is transformed inside the boundaries. (a) Initial transformation guess based on a linear interpolation of the boundaries. Anisotropy reaches 1.41. (b) Without changing the boundaries, the transformation is optimized to minimize the anisotropy of the medium to a maximum of 1.09.

fabrication of inhomogeneous anisotropic media is not yet possible. The fabrication of magnetic materials ($\mu \neq 1$) in the optical regime is also challenging since these are not in general in the form of thin films, compatible with the fabrication process. An additional challenging issue in the design of the structures is the high contrast of refractive indices required by the transformation, which has to be compatible with the fabrication capabilities. We discuss below how these fabrication challenges are overcome.

2.1. Anisotropy

The easiest way to avoid anisotropy is to use conformal transformations, since these are isotropic by nature [19]. Maxwell's fish eye lens is one example of such a transformation. However, designing conformal mappings with a specific goal (such as cloaking, for instance) is challenging and usually leads to extreme values of refractive indices.

Another option to minimize the anisotropy is to specify the transformation only in terms of the shapes (boundaries) of the real and virtual spaces, and numerically optimize the transformation inside the device to make it quasi-conformal. This is accomplished through the minimization of the modified Liao functional of the transformation grid [7]. Once the transformation is quasi-conformal, the resulting media can be approximated by an isotropic medium. Figure 1 below shows an example of such optimization.

2.2. Non-magnetic medium

Since TO is impedance-matched, it requires $\mu'(x, y) = \varepsilon'(x, y)$. If non-magnetic materials are used, another approximation is necessary. In planar devices, as long as $\nabla \mu'(x, y) = \nabla \varepsilon'(x, y)$ is small compared to the wavevector of light, we can specify the medium by an index of refraction $n^2(x, y) = \varepsilon'(x, y)$, i.e., $\mu = 1$. Because TO depends only on the geometries of the virtual and real spaces, the sizes of the devices are not fixed, thus they can be scaled up without changes in the constitutive parameters in order to minimize those gradients as necessary. The drawback of this
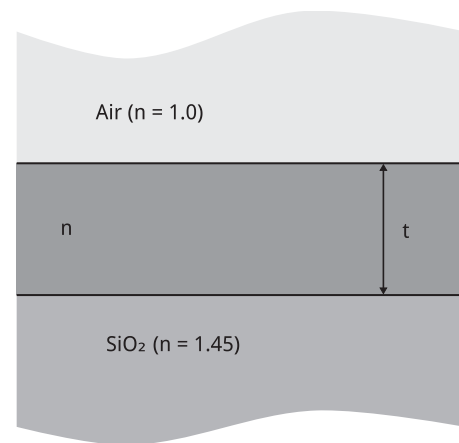

Figure 2. Schematic of an air-cladded slab waveguide on SiO_2 substrate.

approximation is that the boundaries of the device have non-zero reflection coefficients.

2.3. Refractive index map

The refractive index map designed through TO must be constrained to the range of values that can be achieved in thin films (that in turn can be patterned using our fabrication procedure). The choice of working on the Si platform is reasonable since silicon's refractive index ($n_{Si} \approx 3.5$) is among the highest in the optical regime (and thus offers one of the highest contrasts to air or a lower index substrate). Using SiO_2 ($n_{SiO_2} \approx 1.45$) as the substrate for the device layer and air cladding ($n_{air} \approx 1.0$), a slab waveguide is defined by the index of the device layer, as figure 2 shows. For a slowly varying index, this slab can be locally approximated by a homogeneous slab, whose effective index matches the index map prescribed by the TO. Finally, to tailor the effective index of the slab and generate the desired index map, we can either control the index of refraction of the slab or its thickness. For a given thickness t, the maximum effective refractive index available is obtained when the slab is completely filled with Si. The minimum is
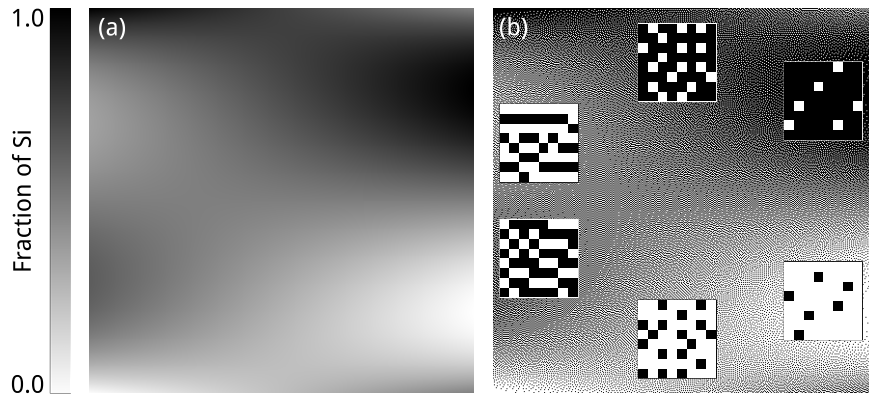
Figure 3. Example of grey-scale map dithering. (a) The grey-scale map $[\rho]_{M,N}$ indicates the volumetric fraction of Si at every point of the device slab. (b) The dithering process quantizes the map into nanometre size regions composed either of Si or air, preserving the overall shades of grey. The insets show regions with $10\times$ magnification.

obtained by decreasing the index of the layer until the slab mode cutoff is reached. The ratio between the maximum and minimum will define the available index contrast for the device fabrication. As an example, for a device layer with 500 nm the possible index contrast is approximately 2:1. The material index of refraction can be directly controlled by the density of silicon in the slab. For example by drilling sub-wavelength holes in the silicon one can decrease the material index of the slab, producing a lower effective index.

We use effective material theory to translate the continuous refractive index map into a discretized version that can be fabricated using nano-lithography. First we sample the refractive index $n(x, y)$ at discrete points and create a density matrix $[\rho]_{M,N}$ for the TE mode through the following relation [20]:

$$\rho_{i,j} = \frac{n^2(id, jd) - 1}{n_{\mathrm{Si}}^2 - 1}, \qquad (1)$$

with $i \in \{1, 2, \ldots, M\}$, $j \in \{1, 2, \ldots, N\}$ and d the feature size chosen for the fabrication of the device (usually between 50 and 120 nm). The effective material theory will only hold if this feature size is smaller than the wavelength. The density matrix is the volumetric fraction of Si in relation to air at each point in the device. It can be seen as a grey-scale image of the device, where values closer to one correspond to regions where the slab is mainly composed of Si, and values closer to zero correspond to regions where the slab is mainly composed of air. Because we already constrained the refractive index map above the cutoff, no region will be actually composed of an air layer.

The second step in discretizing the index map is to quantize $[\rho]_{M,N}$ to values zero, indicating air regions, and one, Si regions of dimensions $d \times d$. This is accomplished through a simple dithering algorithm, commonly used to convert grey-scale images to black and white while visually preserving the shades of grey. Figure 3 shows an example of this process.

The device to be fabricated is directly given by the quantized map: it is composed of a mixture of nanometre size discrete regions of Si and air, positioned so that they effectively constitute the initial grey-scale map and gradient refractive index. Regions with a low refractive index will be essentially

formed by Si pillars surrounded by air, while high refractive index regions will display small air holes in the Si layer. Intermediate regions will vary among these, forming a random checker board-like pattern, as figure 3 shows. One drawback of the dithering method is that the final discrete structures produce high scattering losses, which can be minimized only by decreasing their sizes up to the limits imposed by the fabrication.

2.4. Fabrication

We have optimized the fabrication process for TO-based devices in order to reach a wide range of refractive indices with a 2:1 contrast. The devices are patterned with e-beam lithography over a high resolution XR-1541® resist layer with thicknesses typically between 50 and 200 nm, depending on the requirements for the etch step. The main optimization is on the electron dose used to sensitize the resist: electron backscattering and the width of the electron beam (electron point-spread function) result in what is called the proximity effect. To correct for this effect the electron dose has to be modulated throughout the devices somewhat proportionally to the local shot density (density of silicon pillars).

Once patterned, we etch the silicon layer beneath the resist using a highly anisotropic chlorine process. The result of this process can be seen in figure 4. It is critical to have the correct resist thickness at this stage because regions where holes have to be drilled in the silicon etch much slower than regions where we only need individual silicon pillars. A thicker resist layer allows a longer etch time for better defined holes and correctly etched pillars, but reduces the achievable e-beam resolution. Larger features (larger values of d) help minimize these issues, but produce more light scattering in the final device and degrade the validity of the effective material approximations.

3. Results

Using the dithering method we have demonstrated several TO devices for the optical regime using dielectric materials, including the invisibility cloak, the wavelength independent light concentrator, and a perfect imaging, planar lens.
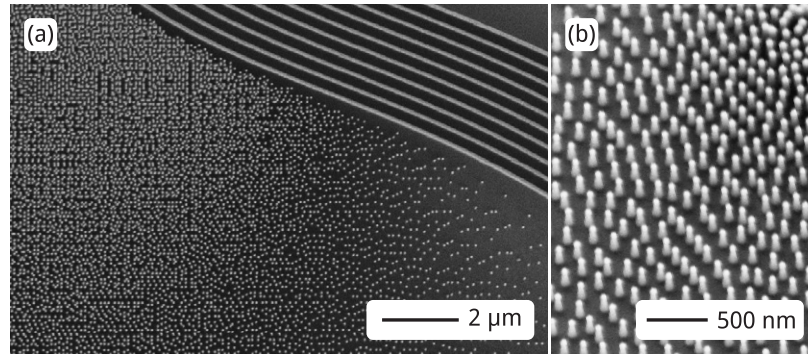
Figure 4. Fabrication of the TO devices. (a) Dithered pattern on silicon showing the different densities of silicon pillars from higher (upper left) to lower (bottom right). The lines on the upper right are a distributed Bragg reflector that was part of this device. (b) Zoomed view of the silicon pillars on an intermediate density region.
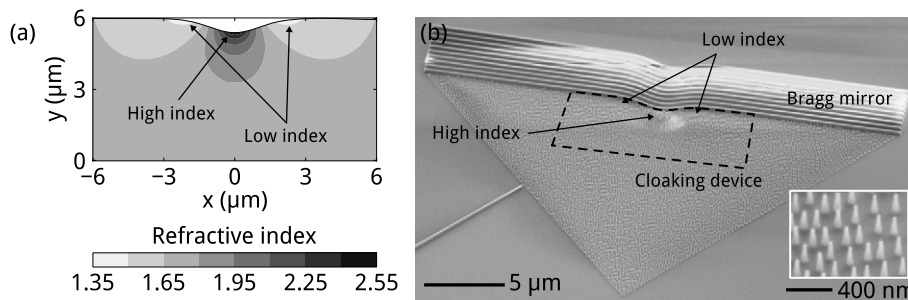

Figure 5. Cloaking device. (a) Initial refractive index map of the cloaking device. (b) SEM image of the fabricated device. The map (a) corresponds to the main cloaking device (dashed area). The inset is a zoomed-in view of the Si nano-structures that compose the device.

3.1. Optical cloaking

An optical cloak can transform the reflection from a deformed mirror into the reflection that would be obtained from a flat mirror. Therefore, for an external observer, the bulge in the mirror surface is invisible. The cloak then creates a hidden chamber behind the deformation that cannot be detected by the observer [7, 9, 10].

The index map required for the cloaking effect contained, after optimization, a residual anisotropic factor of 2%, and an index contrast of about 1.7 [9] that can be achieved using a silicon post top cladded by SiO_2. Figure 5 shows the designed index map, alongside with a scanning electron microscope (SEM) image of the fabricated device.

Experiments showed that the deformed mirror produced a reflection that contained a signature of its deformation. Once the cloaking device was introduced in front of the mirror, this signature disappeared and the reflection was similar to the one coming from a flat mirror [9].

3.2. Light focusing

Because our design process relies only on dielectrics, and not on resonant or highly dispersive materials, the fabricated devices operate at a wide range of frequencies. We have shown using silicon as a platform a broadband light concentrator based on TO [18]: the planar lens, shown in figure 6.

The lens is designed by a transformation that compresses light incident on the input boundary to a small area on the opposing boundary of the lens. The device was left air-cladded to allow the fabrication of a high index contrast, which translates into a higher concentration capability. The simulated power concentration factor was around 2.8. We have experimentally shown the light concentration from this lens using a near-field scanning optical microscope (NSOM) for wavelengths between 1.5 and 1.61 μm.

3.3. Perfect imaging

Maxwell's fish eye is an in-plane lens capable of perfect imaging without the use of negative refraction [21, 22]. Any source point on the surface of the lens produces a perfect image of itself on the opposite side of the lens. The fish eye is based on the conformal mapping of a spherical surface into a plane, thus it does not present any anisotropy. The refractive index map of this device presents a contrast of 2:1. Figure 7 displays an SEM of the fabricated lens on the silicon platform.

The results obtained from this device show that it is possible to obtain sub-diffraction limited images without using negative refraction [16, 17]. The images obtained also show that the discretization of the gradient index into nanometre size structures produces backscattering and is ultimately responsible for the focusing limit of the fish eye.

4. Conclusion

In this paper we show the steps required for implementing TO devices based on dielectric materials. By using numerical
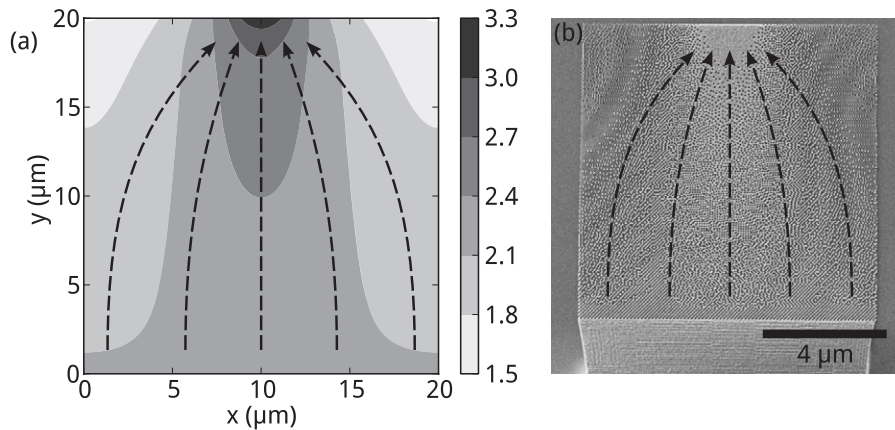
Figure 6. Light concentrator. (a) Refractive index map of the device. Light from the bottom is concentrated towards a tighter spot on the centre of the top edge where the refractive index is higher. (b) SEM image of the fabricated device corresponding to the dithered version of the designed index gradient. The arrows indicate how light travels in the device and concentrates towards the top edge.
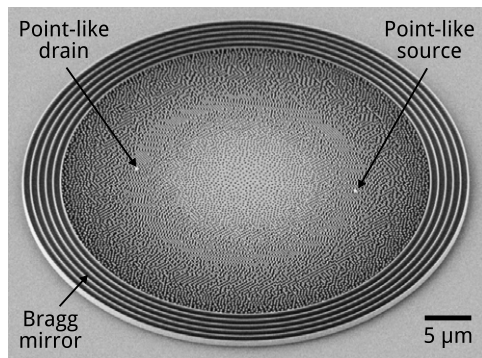

Figure 7. SEM of the fabricated Maxwell's fish eye with a distributed Bragg reflector surrounding it. The source and drain (where the image is formed) are based on gold dots used to scatter light into and out of the device layer.

techniques for conformal mapping and nanometre-patterning we show the ability to tailor the index of refraction of silicon and achieve TO in the optical domain for broadband operation with no fundamental losses. Proximity effect control in e-beam processes as well as the uniform, high aspect ratio etching of different densities of nano-structures in Si are key to decrease their sizes and, consequently, scattering losses in TO devices. In addition we are also investigating smoother index gradient fabrication methods, such as 3d lithography [23] for controlling the index of refraction using the device thickness at the nanometre scale without scattering losses.

References

[1] Leonhardt U and Philbin T G 2006 General relativity in electrical engineering *New J. Phys.* **8** 247
[2] Leonhardt U 2006 Optical conformal mapping *Science* **312** 1777–80
[3] Pendry J B, Schurig D and Smith D R 2006 Controlling electromagnetic fields *Science* **312** 1780–2
[4] Schurig D, Pendry J B and Smith D R 2006 Calculation of material properties and ray tracing in transformation media *Opt. Express* **14** 9794
[5] Shalaev V M 2008 Physics: transforming light *Science* **322** 384–6
[6] Chen H, Chan C T and Sheng P 2010 Transformation optics and metamaterials *Nat. Mater.* **9** 387–96
[7] Li J and Pendry J B 2008 Hiding under the carpet: a new strategy for cloaking *Phys. Rev. Lett.* **101** 203901
[8] Leonhardt U and Tyc T 2009 Broadband invisibility by non-euclidean cloaking *Science* **323** 110–2
[9] Gabrielli L H, Cardenas J, Poitras C B and Lipson M 2009 Silicon nanostructure cloak operating at optical frequencies *Nat. Photon.* **3** 461–3
[10] Valentine J, Li J, Zentgraf T, Bartal G and Zhang X 2009 An optical cloak made of dielectrics *Nat. Mater.* **8** 568–71
[11] Ergin T, Stenger N, Brenner P, Pendry J B and Wegener M 2010 Three-dimensional invisibility cloak at optical wavelengths *Science* **328** 337–9
[12] Pendry J 2000 Negative refraction makes a perfect lens *Phys. Rev. Lett.* **85** 3966–9
[13] Fang N, Lee H, Sun C and Zhang X 2005 Sub-diffraction-limited optical imaging with a silver superlens *Science* **308** 534–7
[14] Kildishev A V and Shalaev V M 2008 Engineering space for light via transformation optics *Opt. Lett.* **33** 43–5
[15] Foca E, Sergentu V V, Daschner F, Tiginynau I M, Ursaki V V, Knöchel R and Föll H 2009 Superlensing with plane plates consisting of dielectric cylinders in glass envelopes *Phys. Status Solidi* a **206** 140–6
[16] Ma Y G, Ong C K, Sahebdivan S, Tyc T and Leonhardt U 2010 Perfect imaging without negative refraction for microwaves arXiv:1007.2530 (July)
[17] Gabrielli L H, Leonhardt U and Lipson M 2010 Perfect imaging in the optical domain using dielectric materials arXiv:1007.2564
[18] Spadoti D H, Gabrielli L H, Poitras C B and Lipson M 2010 Focusing light in a curved-space *Opt. Express* **18** 3181
[19] Leonhardt U and Philbin T 2010 *Geometry and Light: The Science of Invisibility* (New York: Dover)
[20] Nakamura T, Shimizu M, Kimura H and Sato R 2005 Effective permittivity of amorphous mixed materials *Electron. Commun. Japan* Part I **88** 1–9
[21] Leonhardt U 2009 Perfect imaging without negative refraction *New J. Phys.* **11** 093040
[22] Tai C T 1958 Maxwell fish-eye treated by Maxwell equations *Nature* **182** 1600–1
[23] Mosher L, Waits C M, Morgan B and Ghodssi R 2009 Double-exposure grayscale photolithography *J. Microelectromech. Syst.* **18** 308–15